ELSEVIER

LEAFMOD: A New Within-Leaf Radiative Transfer Model

Barry D. Ganapol,[*†] *Lee F. Johnson,*[†‡] *Philip D. Hammer,*[†] *Christine A. Hlavka,*[†] *and David L. Peterson*[†]

We describe the construction and verification of a within-leaf radiative transfer model called LEAFMOD (Leaf Experimental Absorptivity Feasibility MODel). In the model, the one-dimensional radiative transfer equation in a slab of leaf material with homogeneous optical properties is solved. When run in the forward mode, LEAFMOD generates an estimate of leaf reflectance and transmittance given the leaf thickness and optical characteristics of the leaf material (i.e., the absorption and scattering coefficients). In the inverse mode, LEAFMOD computes the total within-leaf absorption and scattering coefficient profiles from measured reflectance, transmittance, and leaf thickness. Inversions with simulated data demonstrate that the model appropriately decouples scattering and absorption within the leaf, producing fresh leaf absorption profiles with peaks at locations corresponding to the major absorption features for water and chlorophyll. Experiments with empirical input data demonstrate that the amplitude of the fresh leaf absorption coefficient profile in the visible wavebands is correlated with pigment concentrations as determined by wet chemical analyses, and that absorption features in the near-infrared wavebands related to various other biochemical constituents can be identified in a dry-leaf absorption profile. ©*Elsevier Science Inc., 1998*

* Departments of Aerospace and Mechanical Engineering, Hydrology and Water Resources, University of Arizona, Tucson

† Ecosystem Science and Technology Branch, NASA/Ames Research Center, California

‡ Institute Earth Systems Science and Policy, California State University, Monterey Bay

Address correspondence to B. Ganapol, Dept. of Aerospace & Mechanical Engineering, Univ. of Arizona, Tucson, AZ 85721. e-mail: ganapol@cowboy.ame.arizona.edu

Received 2 December 1996; revised 18 July 1997.

INTRODUCTION

It is well known that, within plant communities, the leaf is the primary energy harvesting element promoting developmental regulation and adaptive control. The light intercepted and absorbed by the leaf interior, collectively referred to at the canopy level as the fraction of photosynthetically active radiation (FPAR), provides the energy necessary to drive carbon fixation. Previous studies have shown a relationship between canopy near-infrared and red reflectance with FPAR (Asrar et al., 1984; Sellers, 1985). Recently, several ecosystem production models have used remotely sensed data as input for FPAR estimation (Potter et al., 1993; Running and Hunt, 1993; Ruimy et al., 1994; Prince and Goward, 1995).

A portion of the carbon in the litterfall subsequently undergoes decomposition and accompanying nutrient turnover, contributing to the carbon cycle and to gas exchange with the atmosphere. In part, the turnover rates are determined by the foliar biochemical composition. Thus, our ability to predict the dynamics of biogeochemical processes that regulate the ecosystem response to environmental stress would be enhanced if the content of the significant biochemical agents within an ecosystem could be remotely estimated by aircraft or satellite sensors. Toward this end, various empirical studies have investigated the possibility of using airborne imaging spectrometry for biochemical estimation of forest canopies (Peterson et al., 1988; Wessman et al., 1988; Johnson et al., 1994).

Remote estimations of FPAR and biochemistry, however, are sensitive to such factors as sensor calibration, solar irradiance, atmospheric effects, and soil brightness (Goward et al., 1991; Baret and Guyot, 1991). In the case of canopy chemistry, additional uncertainties arise from errors in laboratory measurements of foliar chemis-

REMOTE SENS. ENVIRON. 63:182–193 (1998)

655 Avenue of the Americas, New York, NY 10010

0034-4257/98/$19.00
PII S0034-4257(97)00134-X

try, small sample sizes, and sensor signal-to-noise limitations. To address these complicating factors and to support the use of remote sensing in ecological investigations, there is a continuing need for increased understanding of the fundamental leaf- and canopy-level radiative transfer phenomena.

In this article, we describe a new leaf-level radiative transfer model (LEAFMOD), based on true photon scattering. We begin by introducing the full 3-D radiative transfer equation as an appropriate mathematical model to characterize photon interactions with leaf structure and the leaf biochemicals followed by a brief discussion of previous leaf radiative transfer models. Next, the LEAFMOD description, implementation, and a comparison to a two-stream formulation are given. Then model inversion for extraction of leaf absorption and scattering profiles is considered, with numerical verification and experimental confirmation based on simulated and empirical input data. We end with suggestions for future model development.

Previous Leaf Radiative Transfer Models

The approaches taken by previous leaf radiative transfer modelers fall into two categories: deterministic and probabilistic. In the deterministic models, several fundamental assumptions are required to describe how photons interact with the leaf internal structure and biochemical content. The leaf is assumed to be composed of a continuum of spherical scattering and absorbing centers, each of infinitesimal size, uniformly distributed within a differential leaf volume. The fate of a photon, treated as a "particle fluid," is determined by the relative probabilities of the scattering and absorption interactions occurring within this volume. In addition, the photons move along straight paths between scattering interactions—a phenomenon called photon streaming. The following radiative transfer equation (Chandrasekhar, 1950) describes the energy transfer:

$$\Omega\cdot\vec{\nabla}I(\mathbf{r},\Omega)+\Sigma I(\mathbf{r},\Omega)=\Sigma_s\int_{4\pi}d\Omega' p(\Omega',\Omega)I(\mathbf{r},\Omega'). \quad (1)$$

This equation is a photon energy balance at a position $\mathbf{r}$ in the interior of the leaf. The first term on the left represents the net energy loss from photons moving away from position $\mathbf{r}$ in a direction Ω balanced by the energy loss through absorption and scattering out of direction Ω (second term on the left) and the energy scattered into this direction (term on right). I is the radiance (energy/m^2 s st) at $\mathbf{r}$ of photons traveling in direction Ω within the cone of angles $d\Omega$ (steradians). The scattering phase function p specifies the relative probability of the deflection of a photon from direction Ω' to the cone of directions $d\Omega$ (about Ω). Σ is the total interaction coefficient composed of absorption and scattering coefficients Σ_a and Σ_s, and, since scattering and absorption are independent events,

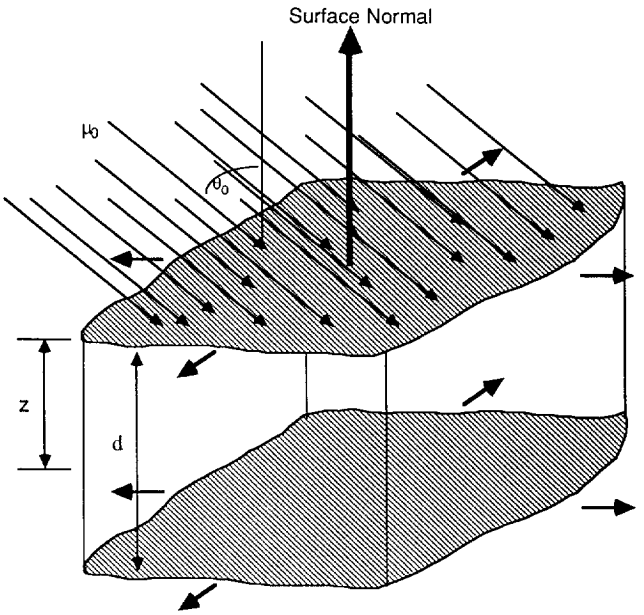

Figure 1. One-dimensional, plane-parallel leaf geometry as assumed by LEAFMOD. μ_0 is the impinging source direction, d is the leaf thickness, and z the longitudinal coordinate measured from the top surface.

$$\Sigma=\Sigma_s+\Sigma_a. \quad (2)$$

In early deterministic models, only two photon directions Ω, away and toward the leaf adaxial (top) surface, were used to characterize the radiative transfer. In this approximation, the so called two-stream or Kubelka–Munk (KM) theory, plane-parallel leaf geometry, as shown in Figure 1, was also assumed. In essence, the radiative transfer equation is transformed into a diffusion equation that was first reported in 1905 and subsequently modified (Kubelka and Munk, 1931; Meador and Weaver, 1979). The solution to the resulting differential equations can be inverted to yield the interaction coefficients Σ_a and Σ_s (Fukshansky, 1992). KM theory tacitly assumes that the radiance is nearly isotropic and that the volume absorption is relatively weak in comparison to the scattering. For this reason, while the simplicity of diffusion theory is rather appealing, errors in the radiance can result at the leaf surfaces, within optically thin media and in regions of high absorption (e.g., in the visible wavebands) (Clark and Roush, 1984).

A significant difficulty of KM theory (or for that matter any radiative transfer formulation) applied to the leaf is the specification of the law of photon deflection (the scattering phase function). To overcome this shortcoming, the plate model (Allen et al., 1970), closely related to the KM model, was developed. In this model, the leaf is assumed to be composed of one or a series of transparent plates with rough Lambertian reflecting surfaces (Jacquemoud and Baret, 1990). Rough surfaces are spec-

ified in order to comply with the assumption of a nearly isotropic radiance in the microlight environment between plates. Using a well-known formulation originated by Stokes (1862), the aggregated reflectance and transmittance of the series of plates can be obtained in closed form in terms of the exitances of a single plate. The plate interaction coefficients can then be calibrated to experimental reflectance and transmittance measurements. The most advanced and successful plate model to date is the PROSPECT model (Jacquemoud and Baret, 1990), in which a structural index N is defined to account for the various plate/air space configurations required to describe the anatomical leaf structure.

The above modeling approaches are to be contrasted with the more complicated but realistic ray tracing methods (Govaerts et al., 1996). These methods are particle simulations that, in the limit of an infinite number of particle trajectories, provide an alternative solution to Eq. (1). Ray tracing models are probably the most realistic but at the same time the most computationally intensive and difficult to numerically implement. In this formulation, photon trajectories (or rays) are followed within a leaf composed of stochastically distributed interacting centers. The photons interact according to the probabilities for scattering and absorption defined along their trajectories. Reflectance and transmittance estimates are obtained after enough trajectories have been followed to reduce uncertainties to a reasonable level. The difficulties in this approach are in generating realistic leaf realizations and inverting for the scattering and absorption coefficients characterizing the biochemical components.

Model Overview

Our overall modeling approach has been to develop a simple model based on the radiative transfer equation as given by the one-dimensional form of Eq. (1) that can be numerically verified and experimentally confirmed. First, we assume a one-dimensional leaf as shown in Figure 1 extending to infinity in the transverse directions. Next, we consider the scattering process producing photon deflection along a trajectory. Scattering is invariably central to any radiative transfer model as well as the most difficult property to characterize properly as evidenced by the earlier model development. Photon deflection into all directions originates primarily from index of refraction discontinuities at cell walls and from diffuse reflection within the microfibril cell wall structure itself (Kerker, 1969; Sinclair et al., 1973). If a nearly random orientation of cell walls is assumed on average, then isotropic scattering (uniform in all directions) is a reasonable approximation. In this way, a consistent particle transport theory treatment of scattering can be constructed without introducing undue complexity and inconsistent ad hoc scattering assumptions. In addition, a homogeneous mixture of (absorbing) biochemicals in the leaf interior will be assumed, with an abaxial (bottom) diffusely reflecting boundary. Leaf surface interactions (other than simple specular reflection) and polarization will not be considered. Our initial investigation will focus on the determination of the scattering and absorption coefficients of a leaf based on laboratory measurements and subsequent model inversions.

LEAFMOD DESCRIPTION

The 1-D Radiative Transfer Equation

The following 1-D radiative transfer equation with longitudinal (z) dependence can be derived by azimuthal integration of Eq. (1):

$$\left[\mu\frac{\partial}{\partial z}+\Sigma\right]I(z,\mu)=\Sigma_s\int_{-1}^{1}d\mu'\, f(\mu',\mu)I(z,\mu'), \tag{4}$$

where I is the radiance for photons traveling in the direction (inclination) range $d\mu$ in the differential volume dz of unit transverse area. The phase function in this formulation has been designated by

$$f(\mu',\mu)$$

[which is the azimuthal average of the general phase function found in Eq. (1)], where μ' is the photon direction [$\mu'=\cos(\theta')$ with θ' relative to the spatial coordinate z measured from the adaxial surface] before collision and μ is the direction after collision. The phase function is normalized such that

$$1=\int_{-1}^{1}d\mu\, f(\mu',\mu). \tag{5}$$

To conform to standard practice and to present a more mathematically convenient form of Eq. (4), the substitution

$$\tau=\Sigma z$$

is introduced, where τ is the optical pathlength measured from the adaxial leaf surface, resulting in

$$\left[\mu\frac{\partial}{\partial\tau}+1\right]I(\tau,\mu)=\frac{\omega}{2}\int_{-1}^{1}d\mu'\, I(\tau,\mu'). \tag{6a}$$

The single scatter albedo ω has been defined as

$$\omega\equiv\Sigma_s/\Sigma. \tag{6b}$$

and the phase function for isotropic scattering,

$$f(\mu',\mu)=1/2, \tag{6c}$$

has been assumed. Equations (6) therefore characterize the azimuthally averaged photon energy transfer within a leaf. We further assume a beam source of strength S_0 illuminates the entire adaxial surface in the direction μ_0; therefore, the appropriate adaxial boundary condition for an azimuthally averaged model is

$$I(0,\mu)=S_0\delta(\mu-\mu_0) \tag{6d}$$

for $\mu>0$. An approximate treatment of surface specular reflection resulting from surface roughness is included by reducing the incident source strength by a factor of

$1-r_{sp}$, where r_{sp} is the specular reflectance of the adaxial surface. If a Lambertian reflecting surface is adjacent to the abaxial surface, then the returned radiance from the abaxial surface to the leaf interior is

$$I(\Delta,-\mu)=2r_s\int_0^1 d\mu'\ \mu' I(\Delta,\mu') \tag{6e}$$

for $\mu>0$, where Δ is the leaf optical thickness defined as Σd_l for an actual leaf thickness d_l. The Lambertian surface is characterized by a reflectance r_s. Note that Eqs. (6) account directly for the incident radiation and its conversion to diffuse radiation. This is in contrast to the equivalent formulation of the transport equation including a first collided diffuse volume source as is often seen in the literature. For our purposes, the primary quantities of interest are the leaf hemispherical reflectance (R_f) and transmittance (T_f)

$$R_f=\frac{1}{\mu_0}\int_0^1 d\mu'\ \mu' I(0,-\mu'), \tag{7a}$$

$$T_f=\frac{1}{\mu_0}\int_0^1 d\mu'\ \mu' I(\Delta,\mu'). \tag{7b}$$

In the above radiative transfer formulation, the variation of the radiance is identical at each optical depth τ in the transverse directions (x and y spatial coordinates), but photon deflection to another path along any trajectory through the leaf is admissible. The details of the solution to Eqs. (6) are outlined in the Appendix with a brief summary given in the following section.

The FN Algorithm

The solution to Eq. (6a) has been the subject of extensive research since the 1950s when Chandrasekhar (1950) popularized the radiative transfer equation for the observation of stellar atmospheres. In general, there is no simple analytical solution. Consequently, many numerical algorithms can be found in the literature (see Ganapol, 1995a,b). As shown in the Appendix, Eq. (6a) can be recast as two (singular) integral equations for the emergent radiances. A convenient numerical solution to these equations, as proposed by Siewert et al. (1986) in his FN algorithm, is the following expansion of the exiting radiances in a set of basis functions $\psi_a(\mu)$ (chosen as the shifted Legendre polynomials in LEAFMOD):

$$I(0,-\mu)=F_R(\mu)e^{-\Delta/\mu}+\frac{\omega}{2}\sum_{a=0}^{N-1} a_a\psi_a(\mu), \tag{8a}$$

$$I(\Delta,\mu)=F_L(\mu)e^{-\Delta/\mu}+\frac{\omega}{2}\sum_{a=0}^{N-1} b_a\psi_a(\mu), \tag{8b}$$

where F_R and F_L are the known impinging (source) radiances at the top and bottom leaf surfaces. a_a and b_a are coupling coefficients to be determined. The appropriate FN order N is determined by iteration when two solutions at consecutive orders are within a desired relative error usually taken to be 10^{-3}. The leading terms in Eqs. (8) represent the unscattered contributions coming directly from the surfaces. The major numerical advantage of this approach is that spatial discretization in optical depth τ is completely avoided, thus reducing the numerical error. Only a quadrature is required to evaluate the matrix elements in our FN formulation. The analytical treatment of the exitances and the subsequent reduction of numerical error makes the FN method a fast and accurate way of solving the radiative transfer equation. Because inversion is required to determine the interaction coefficients, fast execution of a solution algorithm is an essential requirement of an efficient inversion scheme.

Comparison of Transport and KM Theories

A comparison of the reflectances and transmittances given by Eqs. (7) obtained from transport theory and KM theories is shown in Figure 2. A normally incident beam is assumed to impinge on homogeneous isotropically scattering media of three thicknesses [measured as an optical thickness (Δ)] and the response as a function of the single-scatter albedo ω is observed. Since the single-scatter albedo is a ratio of the probability of scattering to the total interaction probability (absorption plus scattering) for a photon interaction, $\omega=\Sigma_s/\Sigma$, ω is a measure of the diffuse scattering nature of the medium. As the medium becomes more highly scattering (single scatter albedo approaches 1), Figures 2a,b show that the reflectance and transmittance of KM theory approaches the exitances of transport theory. Clearly, KM theory is in error for highly absorbing media for which the single scatter albedo is less than about 0.7, especially for thicker media, which is also supported by previous investigations (Clark and Roush, 1984). The primary reason for the large discrepancy is that the radiance distribution assumed by KM theory admits only a linear variation in the photon direction. This is a poor approximation in a highly absorbing medium since the scattering is insufficient to redistribute monodirectional photons from the source uniformly to all directions. For the thin medium, both the reflectance and transmittance (as displayed in Figs. 2a,b) are remarkably accurate, most likely a result of the reduced amount of total absorption for this case. A comparison of the exiting radiance distributions from transport theory and KM theory is shown in Figures 2c,d for a highly scattering medium of $\omega=0.95$ and an optical thickness of 10. The linear approximation of KM theory is readily apparent for the reflected radiance in comparison to its true variation. The transmitted radiance is nearly linear as predicted by KM theory but of a different slope from that obtained by transport theory.

INVERSION PROCEDURES

Exact Inversion

With an approximate solution to the radiative transfer equation now in place, we can turn our attention to the

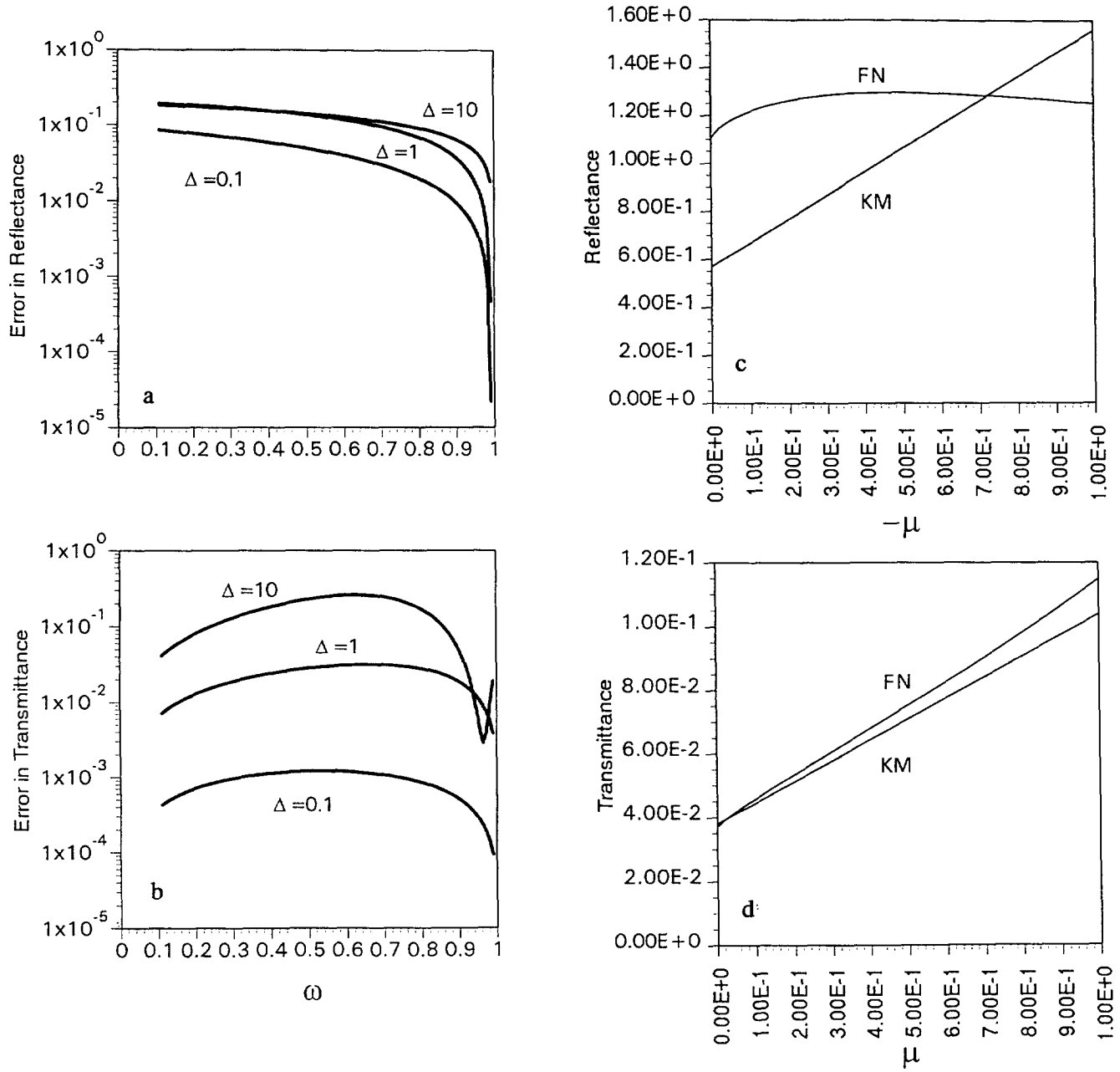

Figure 2. a,b) Variation of the relative error $[|I_{FN}-I_{KM}|/I_{FN}]$ with the leaf albedo (ω) for reflectances and transmittances as obtained from transport (FN) and KM theories for optical thicknesses Δ=0.1, 1, 10. Relatively large discrepancies occur for highly absorbing (ω<0.7) and optically thick (Δ=10) media. c,d) Exiting radiance distributions for an optically thick (Δ=10), highly scattering medium (ω=0.95), as obtained from transport (FN) and KM theories. The linear approximation of KM is apparent in the reflectance, whereas KM theory more closely approximates the transmittance of transport theory.

determination of leaf total absorptivity profile as represented by the absorption coefficient Σ_a in the transport equation. To obtain the leaf absorption coefficient, an estimate of the scattering coefficient Σ_s is required. As noted from the previous discussion, these physical parameters are intimately intertwined in the exitances as represented by Eqs. (7). Here, we take an approach in which the transport solution is viewed as having two unknown coefficients, Σ_a and Σ_s, at each wavelength. Therefore, if we have two leaf experimental measurements, say of the reflectance $[R_f(\text{exp})]$ and transmittance $[T_f(\text{exp})]$ at a specified number of wavelengths λ, then, at each wavelength, we can require the model to faithfully reproduce these measurements as follows:

$$R_f(\text{exp})=R_f(\Sigma_a,\Sigma_s), \tag{10a}$$

$$T_f(\text{exp})=T_f(\Sigma_a,\Sigma_s). \tag{10b}$$

Table 1. Input Parameters Required for LEAFMOD Exact Inversion

Parameter	*Definition*
r_{sp}	Specular reflectance of top surface
r_s	Reflectance of adjacent bottom surface
d_l	Average leaf thickness
R_f	Reflectance measurement at λ_i
T_f	Transmittance measurement at λ_i
e_R	Desired relative error
λ_i	Desired wavelengths
L_{max}	Maximum number of desired wavelengths

A measured leaf thickness d_l is also required. $R_f(\Sigma_a,\Sigma_s)$ and $T_f(\Sigma_a,\Sigma_s)$ are determined from the calculated radiances and are given by Eqs. (7). Table 1 shows the other necessary input parameters required for the model inversion. Note that for a given leaf thickness there are two equations for the two unknown interaction coefficients (Σ_a and Σ_s) and the system is, in principle, completely determined. Equations (10) therefore constitute an "exact inversion" because the number of unknowns is the same as the number of equations. Interaction coefficients, however, enter into the FN solution in a highly nonlinear fashion through the leaf optical depth and the single scatter albedo. For this reason, there are some additional considerations. A solution to a set of highly nonlinear equations is required and, consequently, the question of existence and uniqueness of the solution should be addressed. In general, there is no guarantee that these equations have just one solution or, for that matter, have any solutions at all. From our experience, however, either no solution exists because of unphysical constraints or only one solution exists.

A globally convergent multiple root solver is used to solve Eqs. (10) for the interaction coefficients. A global method is an iterative root searching procedure featuring convergence to a set of roots regardless of the initial guess. The Newton–Raphson iterative global scheme, as found in Press et al. (1992), was adapted for the inversion. The method is based on the multivariate Newton–Raphson equation solver with an estimate to a set of roots obtained from a gradient chosen to ensure a path in the parameter space directed toward a global minimum. A gradient of the solution with respect to the desired parameters (Σ_a and Σ_s) is obtained from an efficient finite difference approximation. Failure of the Newton–Raphson equation solver is possible when a local minimum is reached. An error caution is indicated if such a minimum is encountered.

Approximate Inversion

The inversion procedure described above is completely determined when both exitance measurements are available. However, the procedure becomes problematic when either R_f or T_f are unavailable. Such is the case with the NIRS Systems Model 6500 spectrophotometer (NIRS Systems Inc., Silver Spring, Maryland) as configured at NASA/Ames Research Center, which measures R_f only; this is generally the case in the remote sensing context as well. In order to perform initial experiments to exercise LEAFMOD, an "approximate inversion" was constructed. To establish the inversion procedure, additional information must be supplied to offset the loss of one measurement. Thus, a modeling conjecture to account for the missing information of the reflectance measurement was imposed. Since scattering is primarily controlled by the variation of index of refraction at cell wall/air or water interfaces and cell wall scattering, the anatomical cellular structure of leaves is relatively similar. Considering this similarity, to a first approximation, the scattering coefficient for a given species applies to another leaf of the same or a morphologically similar species after an adjustment for the difference in the density of interfacial scattering centers. While this conjecture is not entirely justifiable (and therefore we attempt no proof), it does allow for the initiation of modeling testing and, therefore, was made primarily in the interest of advancing the modeling effort. Thus, if Σ_{s1} is known from measurements performed on species 1 of known cell wall density N_1, the appropriate approximation for the scattering coefficient for species 2 of cell-wall density N_2 will be

$$\Sigma_{s2}=\Sigma_{s1}\left[\frac{N_2}{N_1}\right]. \tag{11}$$

In this study, neither N_1 nor N_2 were known and therefore they were assumed equal for the morphologically similar cases investigated. It should be noted that the ratio Σ_{s2}/Σ_{s1} plays a similar role to the parameter N of previous leaf models (see Allen et al., 1969).

In effect, the above conjecture allows the separation of the scattering and absorption processes. Scattering is assumed to be a consequence of the leaf anatomical structure as influenced by the cell walls, whereas absorption takes place through the specific biochemicals and water distributed within a cell. With a predetermined scattering coefficient for species 2, only Eq. (10a) need be solved to provide an estimate of the absorption coefficient Σ_{a2}.

NUMERICAL VERIFICATION

The exact and approximate inversions incorporating the (forward) FN solution have been coded in a FORTRAN 77 program called LEAFMOD. As with any algorithm, algorithmic development does not stop with the writing of code. A necessary step in the code development process is to provide the user with the assurance of proper operation. Often, confirmation of an algorithm involves verification that the numerical method has been properly coded and performs as expected and that the results are intuitively reasonable. For this reason, several numerical

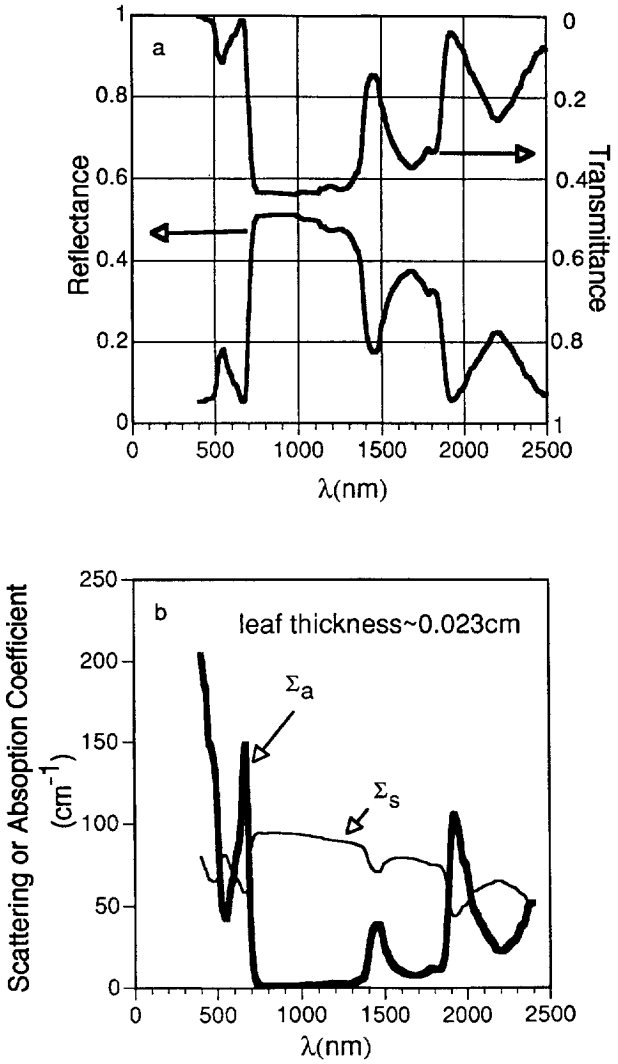

Figure 3. a) Leaf reflectance and transmittance versus wavelength (nm) obtained from the PROSPECT model for green soybeans (after Jacquemoud and Baret, 1990). b) Scattering (Σ_s) and absorption (Σ_a) coefficient profiles derived by LEAFMOD exact inversion on curves in a).

verification exercises for the LEAFMOD code are discussed in this section.

Inversion Stability

Reflectance and transmittance measurements for a green soybean leaf (Fig. 3a), were simulated by the established PROSPECT model. A leaf thickness of 0.023 cm was implied from the specified (Jacquemoud and Baret, 1990) equivalent water thickness (d_{H2O}) and by assuming the leaf was 67% hydrated ($h_{\%}$) which is typical of dicot leaves [$d_l = d_{H2O}/(0.01 h_{\%})$]. These simulated measurements were then introduced into the LEAFMOD exact inversion with a non reentrant boundary condition [$r_s = 0$] on the abaxial surface and a desired relative error of 0.001 for the exitances.

The resulting absorption and scattering profiles were obtained in absolute units of (fractional probability of interaction)/pathlength (cm^{-1}) as shown in Figure 3b. The absorption spectrum in the visible wavebands has the appropriate peaks and shoulders at the wavelengths corresponding to the influence of chlorophyll a and b. The absorption spectrum in the NIR is representative of water where little absorption occurs in the range 800 nm$<\lambda<$1350 nm and major absorption peaks exist at about 1450 nm and 1950 nm.

The variation of the scattering coefficient with wavelength is also reasonable in that it generally follows the variation of the average leaf refractive index with wavelength (Allen et al., 1970) except at the chlorophyll and water absorption peaks. The influence of these strong absorption peaks on the scattering coefficient is not entirely unexpected because of the intimate coupling of the scattering and absorbing effects in the transport equation. The abrupt features in the scattering profile near the water absorption peaks have previously been reported (Allen et al., 1970; 1969). While the concept of photon deflection resulting from changes in the index of refraction has been used to justify the scattering source in the radiative transfer equation, the scattering interaction coefficient in the transport formulation is distinct from the index of refraction. The scattering interaction coefficient represents a volume averaged scattering effect while deflection through the refractive index represents a microscopic effect. The volumetric scattering and absorption coefficients are spatial averages of the refractive scattering occurring at cell walls and absorption within the cell walls. In a transport formulation, these events occur in the same differential volume and therefore cannot be separated entirely. For this reason, the scattering interaction coefficient cannot be strictly interpreted as directly proportional to the index of refraction.

To provide a test of the numerical stability of the approximate inversion, the soybean absorption spectrum Σ_a shown in Figure 3b was arbitrarily multiplied by the factors $f=0.5$, 1.1, and 2 to form the modified absorption coefficient $\Sigma_a' = f\Sigma_a$. With the scattering coefficient spectrum of Figure 3b held fixed, the corresponding reflectance and transmittance spectra were then determined from the FN transport solution for these cases from LEAFMOD run in the forward mode. Subsequently, each reflectance spectrum was input into the approximate inversion algorithm as a simulation of a reflectance measurement in Eq. (10a) along with the (unmodified) soybean reference scattering profile, and the absorption coefficient (now known to be a multiple of the original spectrum) was obtained by inversion. A comparison of the resulting absorption coefficient profiles and the modified absorption coefficient profiles then provides an assessment of how faithful the inversion process is. When the resulting absorption profiles were proportioned as

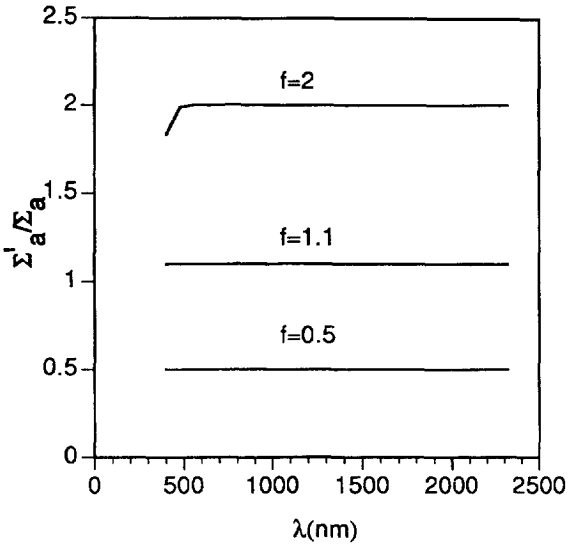

Figure 4. As a measure of the stability of the approximate inversion, Σ_a of Figure 3b was multiplied by the indicated factors f, and the corresponding reflectance and transmittance spectra were then obtained for each case from LEAFMOD run in foward mode. The reflectance spectrum and (unmodified) scattering coefficient profile were input to the approximate inversion to recover the modified absorption profile Σ_a'. Note the near-perfect correspondence between factors f and Σ_a'/Σ_a, indicating the stability of the approximate inversion algorithm.

shown in Figure 4, almost perfect recovery of the multiplicative factors (f) was observed across the entire spectrum, indicating the stability and the robustness of the approximate inversion.

Forward Peaked Scattering Equivalence

A test of the exact inversion procedure is provided by a modification of the scattering kernel to include a purely forward peaked component. If the deflection law is assumed to be composed of an isotropic scattering component and a component for photons that are not deflected at all, the phase function becomes

$$f(\mu',\mu)=\frac{1-\beta}{2}+\beta\delta(\mu-\mu') \tag{12}$$

with the normalization given by Eq. (5) satisfied. β represents the fractional probability of forward directed scattering. When this phase function is introduced into Eq. (4), we find, after some manipulation,

$$\left[\mu\frac{\partial}{\partial\tau'}+1\right]I'(\tau',\mu)=\frac{\omega'}{2}\int_{-1}^{1}d\mu'\,I'(\tau',\mu'), \tag{13}$$

where in terms of the original scattering interaction coefficient, the modified scattering interaction coefficients become

$$\Sigma_s'=(1-\beta)\Sigma_s, \tag{14a}$$

$$\Sigma'=\Sigma-\beta\Sigma_s=\Sigma_a'+\Sigma_s', \tag{14b}$$

giving for the optical depth

$$\tau'=\Sigma' x. \tag{14c}$$

The single-scatter albedo then becomes

$$\omega'=\frac{(1-\beta)\omega}{1-\omega\beta}. \tag{14d}$$

Since the inclusion of a purely straight-ahead component in the phase function physically only effects the scattering properties of the medium, we expect the absorption to be unaffected as is theoretically verified by Eq. (14b), giving

$$\Sigma_a=\Sigma_a'. \tag{15c}$$

From Eq. (14a), the scattering, in this case, adjusts according to

$$\Sigma_s'=\Sigma_s/(1-\beta). \tag{16}$$

This is exactly what is observed when the PROSPECT reflectance and transmittance data of Figure 3a are again used to obtain the absorption profile for the soybean leaf from the exact inversion for several values of β. The independence of the absorption profile from β was verified to within the desired relative error for β=0.5 and 0.9 as required by theory. This provides further evidence of the stability and proper coding and operation of the inversion algorithms. In addition, this test indicates an insensitivity of the absorption profile to the anisotropy of scattering.

EXPERIMENTAL CONFIRMATION

Sample Thickness and Moisture Status

A leaf stacking and drying experiment was performed on the NASA/Ames NIRS6500 spectrophotometer equipped with the Spinning Sample Module and Standard Cup. Bidirectional reflectance measurements were made of stacks of one to six fresh *Prunus lyonii* (Catalina cherry) leaf punches (~3.5 cm diameter). The leaves were then oven-dried (at 33°C), and reflectance measurements were made intermittently during the next nine days. Reflectance measurments, shown in Figure 5, were taken over the 400 nm<λ<2500 nm range, with 10 nm bandwidth and 2 nm sampling interval. Illumination was normal to the sample and reflected energy was recorded by detectors at a 45° view zenith angle. The sample was rotated azimuthally during measurement. Absolute reflectance was inferred by comparison to a ceramic standard of known reflectance. Sixteen scans were acquired and averaged per sample. In addition, reflectance of the background surface was measured (<4%, 400–2500 nm) and input into the model as r_s.

Since only the reflectance measurement was available, the approximate inversion (with Σ_s from the fresh soybean reference leaf of Fig. 3b) was used to determine

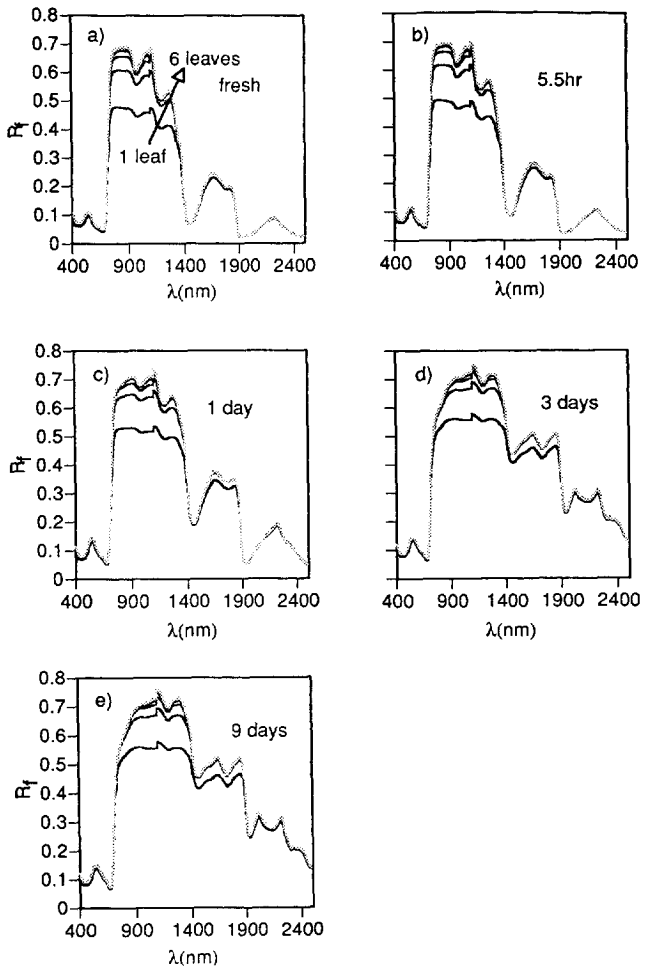

Figure 5. Bidirectional reflectance measurements made by NIRS6500 spectrophotometer on stacks of *Prunus lyonii* leaves, ranging in thickness from one to six leaves. Drying times in oven at 33°C are indicated. Note reflectance increase with stack depth in regions of high scatter (~800–1300 nm, ~1500–1800 nm).

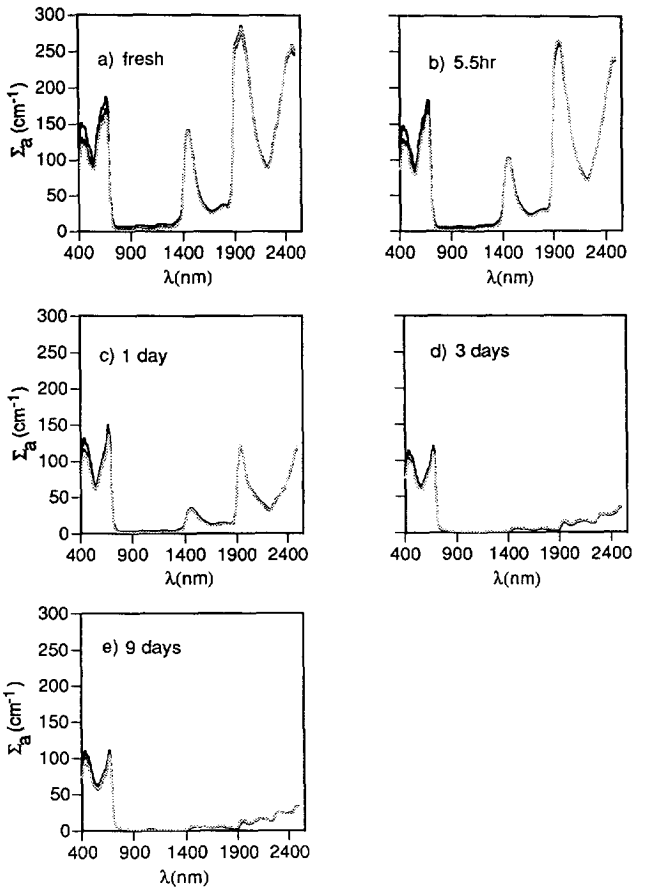

Figure 6. Absorption profiles derived by LEAFMOD approximate inversion for the reflectances of Figure 5. As observed, sample thickness has little effect on profile amplitude.

absorption profiles under all moisture conditions and sample thicknesses as shown in Figure 6. At each time interval the thickness of the top leaf punch was measured at several locations and determined as the average of the interveinal and midrib values. The total thickness of each sample was estimated as the top punch thickness multiplied by the number of punches in the stack. The following remarks concerning the spectra of Figures 5 and 6 are relevant:

1. Compared to reflectance spectra in the 800–1300 nm and 1500–1800 nm regions, the absorption profile amplitudes are relatively independent of sample thickness. This finding provides evidence that the model separates the effects of scattering from absorption, at least to a first approximation.
2. A reduction of water absorption features (centered at ~1400 nm and ~1900 nm) with dryout is clearly seen in the reflectance and absorption spectra. Spectra at 3 days are representative of a dried leaf.
3. At 1 day of drying and thereafter, there is an increase in reflectance and reduction in the absorption in the visible region, possibly resulting from thermally induced reorientation of absorbers and changes in chemical composition and surface roughness not modeled.
4. Spectral features are apparent in the 9-day absorption profiles shown in Figure 7. Various near-infrared absorption features attributable to the biochemical constituents of lignin, cellulose, and protein can be identified. While these features can also be detected in the reflectance spectra, here they appear isolated from the scattering effect and are given in terms of absolute pathlength units.

From this exercise, we conclude overall that the LEAFMOD approximate inversion generates intuitively reasonable results for the estimation of the leaf absorption coefficient with wavelength. From the numerical point of

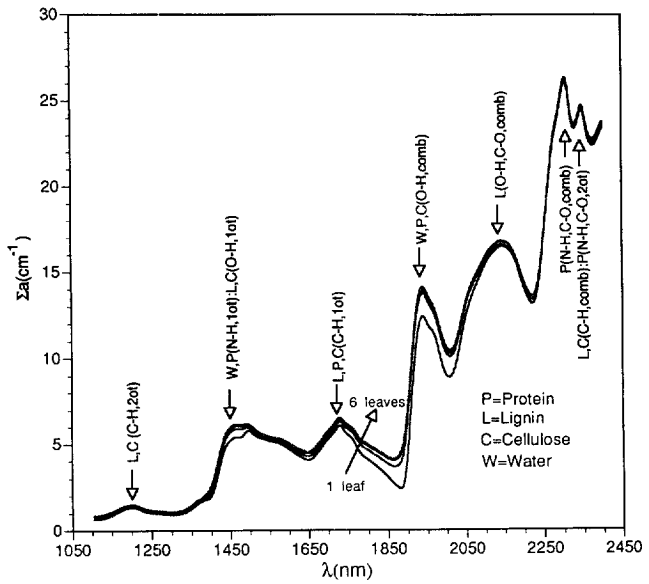

Figure 7. Rescaling of Figure 6e, with identification of absorption features possibly attributable to protein (P), lignin (L), cellulose (C) and water (W). Attributions after Osborne et al. (1993) and Williams and Norris (1987). Some associated organic bonds are also shown in parentheses.

view, the Newton–Raphson root solver always converged to appropriate roots and never to a local minimum.

Response to Pigment Concentrations

The LEAFMOD exact inversion was performed on spectral measurements from the Leaf Optical Properties Experiment (LOPEX) archive (Hosgood et al., 1995) to examine the Σ_a response to pigment (total chlorophyll+carotenoids) concentration. The inversion was applied to R_f and T_f (over 400–800 nm) of 280 fresh, single leaves: five replicates from each of 56 samples (44 dicot, 12 monocot). A total of 38 tree and crop species were represented; leaf thickness ranged from 0.0086 cm to 0.0583 cm.

The mean absorption profile amplitude in the 450–680 nm region was significantly (0.01 level) correlated with pigment mass cm^{-3} fresh leaf volume (r=0.75) and also g^{-1} fresh leaf weight (r=0.67), as determined by conventional laboratory methods used for the LOPEX data. A strong correlation was observed throughout the spectral region in both cases, in the former case ranging from a minimum of ~0.63 at 680 nm to >0.80 in the 525–560 nm region. As chlorophyll and carotenoids are the major absorbers of visible region energy, this exercise provides evidence of linkage between absorber concentration and Σ_a amplitude. Possibly due to the confounding effect of scattering differences among these diverse samples, no significant correlation was seen between R_f or T_f and either expression of pigment concentration. This observation provides evidence of the ability of LEAFMOD, by controlling for scatter, to enhance information on absorbing properties of the leaf.

CONCLUSIONS AND FUTURE EFFORT

A radiative transfer model, LEAFMOD, has been developed to simulate the photon scattering and absorbing processes within a leaf. LEAFMOD is based on the solution (by the FN method) of the one-dimensional radiative transfer equation. Through the FN method, the radiative transfer equation is reformulated as two integral equations for the surface radiances. The corresponding solution is approximated by an expansion in a set of N basis functions where the expansion coefficients are obtained by collocation and subsequent matrix inversion. N is increased until the desired convergence is achieved. From this solution, the angular radiance distribution in the leaf interior can also be obtained, which may prove useful in future studies of the radiative transfer properties of the within-leaf microlight environment (Vogelmann, 1989). The absorption and scattering profiles are obtained through model inversion. An exact procedure uses the reflectance and transmittance measurements at each wavelength to generate a consistent set of equations for these profiles. For testing purposes, an approximate inversion procedure has also been established based on a reflectance measurement only.

Model verification showed that 1) the fresh-leaf absorption profile has features corresponding to water and chlorophyll, while the scattering profile generally follows variation of the leaf refractive index with wavelength, 2) the inversion is stable, and 3) the absorption profile seems to be unaffected by relaxation of the isotropic scattering assumption in the phase function. Exercises with empirical data showed that 1) LEAFMOD effectively separates the effects of scattering and absorption, 2) near-infrared absorption features associated with leaf constituents other than water are identifiable in the dry-leaf absorption profile, and 3) the amplitude of the absorption coefficient profile in the visible region is sensitive to the pigment concentration of fresh leaves.

We further intend to analyze the model sensitivity to relaxation of various modeling assumptions, including those of isotropic scattering and a homogeneous medium. Here, the transport model has a distinctive advantage over KM theory. A highly anisotropic scattering leaf phase function can be considered if necessary, whereas, at most, only linearly anisotropic scattering can be considered with KM theory. Another major focus will be on simulation of the effects of leaf chemistry on leaf reflectance, and evaluation of analytical techniques to estimate component concentrations from leaf spectra. Longer term issues concern the two- and three-dimensionality of leaves, the stochastic nature of the distribution of absorbing and scattering elements, and linkage of LEAFMOD to a canopy model through the leaf phase function.

B. D. G. gratefully acknowledges the support of the National Academy of Science as a National Research Council Associate at

NASA/Ames Research Center during the completion of this work. Further support was provided by NASA's Terrestrial Ecology Program as UPN:462-61-10-10. The LOPEX dataset was established during an experiment conducted by the Advanced Techniques Unit of the Institute for Remote Sensing Applications/Joint Research Center of the European Commission. We wish to thank S. Jacquemoud for access to the PROSPECT program. Finally, we thank the two reviewers for their careful review of the manuscript and many helpful suggestions for improvement.

APPENDIX: A REVIEW OF THE FN METHOD

To begin the solution method, Eq. (6a) is rewritten with μ replaced by $-\mu$, multiplied by $e^{-\tau/s}$ and then integrated over τ on $[0,\Delta]$ and over μ on $[-1,1]$ to give for $Re(s)>0$

$$\int_{-1}^{1} d\mu \frac{\mu}{\mu-s} C(\mu,s)=\Lambda(s)\frac{I^*(s)}{s}, \tag{A1a}$$

where

$$\Lambda(s)=1-\frac{s\omega}{2} ln\left[\frac{s+1}{s-1}\right], \tag{A1b}$$

$$C(\mu,s)=I(0,-\mu)-I(\Delta,-\mu)e^{-\Delta/s}, \tag{A1c}$$

and

$$I^*(s)=\int_0^{\Delta} d\tau\, e^{-\tau/s}\int_{-1}^{1} d\mu\, I(\tau,-\mu). \tag{A1d}$$

To obtain a second equation, replace s by $-s$ and μ by $-\mu$ in Eq. (A1a) and multiply by $e^{-\Delta/s}$ to give for $Re(s)>0$

$$\int_{-1}^{1} d\mu \frac{\mu}{\mu-s} D(\mu,s)=\Lambda(s)\frac{J^*(s)}{s}, \tag{A2a}$$

where

$$D(\mu,s)=I(\Delta,\mu)-I(0,\mu)e^{-\Delta/s}, \tag{A2b}$$

$$J^*(s)=\int_0^{\Delta} d\tau\, e^{-(\Delta-\tau)/s}\int_{-1}^{1} d\mu\, I(\tau,-\mu). \tag{A2c}$$

In addition, since $\Lambda(v_0)$ satisfies the dispersion relation

$$\Lambda(v_0)=0, \tag{A3}$$

for $s=v_0$, Eqs. (A1a) and (A2a) also satisfy

$$\int_{-1}^{1} d\mu \frac{\mu}{\mu-v_0} C(\mu,v_0)=0, \tag{A4a}$$

$$\int_{-1}^{1} d\mu \frac{\mu}{\mu-v_0} D(\mu,v_0)=0. \tag{A4b}$$

From the Plemelj relations (Roos, 1969), these equations can be manipulated to give

$$v\lambda(v)C(v,v)=\frac{\omega v}{2}\int_{-1}^{1} d\mu \frac{\mu}{\mu-v} C(\mu,v), \tag{A5a}$$

$$v\lambda(v)C(v,v)=\frac{\omega v}{2}\int_{-1}^{1} d\mu \frac{\mu}{\mu-v} D(\mu,v), \tag{A5b}$$

where

$$\lambda(v)=1-\frac{\omega v}{2} ln\left[\frac{1+v}{1-v}\right]. \tag{A5c}$$

When C and D are expressed in terms of the reflected and transmitted intensities, we have

$$v\lambda(v)I(0,-v)-\frac{\omega v}{2}\int_0^1 d\mu\frac{\mu}{\mu-v}I(0,-\mu)+\frac{\omega v}{2}e^{-\Delta/v}\int_0^1 d\mu\frac{\mu}{\mu+v}I(\Delta,\mu)$$
$$=\frac{\omega v}{2}\int_0^1 d\mu\frac{\mu}{\mu+v}F_L(\mu)+e^{-\Delta/v}\left\{v\lambda(v)F_R(v)-\frac{\omega v}{2}\int_0^1 d\mu\frac{\mu}{\mu-v}F_R(\mu)\right\}, \tag{A6a}$$

$$v\lambda(v)I(\Delta,-v)-\frac{\omega v}{2}\int_0^1 d\mu\frac{\mu}{\mu-v}I(\Delta,-\mu)+\frac{\omega v}{2}e^{-\Delta/v}\int_0^1 d\mu\frac{\mu}{\mu+v}I(0,\mu)$$
$$=\frac{\omega v}{2}\int_0^1 d\mu\frac{\mu}{\mu+v}F_R(\mu)+e^{-\Delta/v}\left\{v\lambda(v)F_L(v)-\frac{\omega v}{2}\int_0^1 d\mu\frac{\mu}{\mu-v}F_L(\mu)\right\}, \tag{A6b}$$

where the boundary conditions on the adaxial (L) and abaxial (R) surfaces are given by

$$F_L(\mu)=\delta(\mu-\mu_0), \tag{A7a}$$

$$F_R(\mu)=2r_s\int_0^1 d\mu'\,\mu' I(\Delta,\mu'). \tag{A7b}$$

If the expressions of Eqs. (8) are introduced into Eqs. (A6) with N values of v_β, $\beta=0,1,\ldots N-1$, the following $2N$ equations will result:

$$\sum_{\alpha=0}^{N-1}\left[a_\alpha B_{\alpha\beta}+b_\alpha A_{\alpha\beta}e^{-\Delta/v_\beta}\right]=R_{1\beta}(\Delta), \tag{A8a}$$

$$\sum_{\alpha=0}^{N-1}\left[a_\alpha A_{\alpha\beta}e^{-\Delta/v_\beta}+b_\alpha B_{\alpha\beta}\right]=R_{2\beta}(\Delta), \tag{A8b}$$

where $R_{1\beta}$ and $R_{2\beta}$ can be expressed in terms of the boundary conditions. The v_β's are chosen to be the zeros of the shifted Legendre polynomial of degree $N-1$ plus the zero of the dispersion relation [Eqs. (A5)]. $A_{\alpha\beta}$ and $B_{\alpha\beta}$ are the matrix elements and integrals over known integrands which are numerically evaluated by a shifted Gauss/Legendre quadrature. Of note is the dependence of $R_{1\beta}$ and $R_{2\beta}$ on the boundary conditions, which may, in turn, depend on the intensities being sought [see Eq. (6e), for instance]. An iterative process can then be used to maintain the symmetry of Eqs. (A8). The $2N$ equations given by Eqs. (A8) are then solved by matrix inversion to give the coupling coefficients a_α and b_α. Finally, an outer iteration is imposed on the order N to ensure a desired accuracy.

REFERENCES

Allen, W. A., Gausman, H. W., Richardson, A. J., and Thomas, J. R. (1969), Interaction of isotropic light with a compact plant leaf. *J. Opt. Soc. Am.* 59:1376–1380.

Allen, W. A., Gaussman, H. W., and Richardson, A. J. (1970),

Mean effective optical constants of cotton leaves. *J. Opt. Soc. Am.* 60:542–547.

Asrar, G., Fuchs, M., Kanemasu, E. T., and Hatfield, J. L. (1984), Estimating absorbed photosynthetic radiation and leaf area index from spectral reflectance in wheat. *Agron. J.* 76:300–306.

Baret, F., and Guyot, G. (1991), Potentials and limits of vegetation indices for LAI and APAR assessment. *Remote Sens. Environ.* 35:161–173.

Chandrasekhar, S. E. (1950), *Radiative Transfer*, Oxford University Press, London.

Clark, R. N., and Roush, T. L. (1984), Reflectance spectroscopy: quantitative analysis techniques for remote sensing applications. *J. Geophys. Res.* 89:6329–6340.

Fukshansky, L. (1992), Photon transport in leaf tissue. In *Applications in Plant Physiology* (J. Ross and R. Myneni, Eds.).

Ganapol, B. (1995a), Radiative transfer in a semiinfinite medium with a specularly reflecting boundary. *J. Quant. Spectrosc. Radiat. Transfer* 33:257–270.

Ganapol, B. (1995b), The Milne problem for a specularly reflecting boundary. *J. Quant. Spectrosc. Radiat. Transfer* 54: 795–805.

Govaerts, Y. M., Jacquemoud, S., Verstraete, M. M., and Ustin, S. L. (1996), Three-dimensional radiation transfer modeling in a dicotyledon leaf. *Appl. Opt.* 35:6585–6598.

Goward, S. N., Markham, B., Dye, D. G., Dulaney, W., and Yang, J. (1991), Normalized difference vegetation index measurements from the Advanced Very High Resolution Radiometer. *Remote Sens. Environ.* 35:257–277.

Hosgood, B., Jacquemoud, S., Andreoli, G., Verdebout, J., Pedrini, G., and Schmuck, G. (1995), Leaf Optical Properties Experiment 93 (LOPEX93), Report EUR-16095-EN, European Commission, Joint Research Centre, Institute for Remote Sensing Applications, Ispra, Italy.

Jacquemoud, S., and Baret, F. (1990), PROSPECT: a model of leaf optical properties spectra. *Remote Sens. Environ.* 34: 75–91.

Johnson, L. F., Hlavka, C. A., and Peterson, D. L. (1994), Multivariate analysis of AVIRIS data for canopy biochemical estimation along the Oregon Transect. *Remote Sens. Environ.* 47:216–230.

Kerker, M. (1969), *The Scattering of Light and Other Electromagnetic Radiation*, Academic, New York.

Kubelka, P., and Munk, F. (1931), Reflection characteristics of paints. *Z. Tech. Phys.* 12(11a):593–601.

Meador, W. E., and Weaver, W. R. (1979), Diffuse approximation for large absorption in radiative transfer. *Appl. Opt.* 18:1204–1208.

Osborne, B. G., Fearn, T., and Hindle, P. H. (1993), *Practical NIR Spectroscopy with Applications in Food and Beverage Analysis*, Longman Scientific, Essex, U.K., Chap. 2.

Peterson, D. L., Aber, J. D., Matson, P. A. et al. (1988), Remote sensing of forest canopy and leaf biochemical contents. *Remote Sens. Environ.* 24:85–108.

Potter, C. S., Randerson, J. T., Field, C. B., et al. (1993), Terrestrial ecosystem production: a process model based on global satellite and surface data. *Global Biogeochem. Cycles* 7:811–841.

Press, W., et al. (1992), *Numerical Recipes*, Cambridge University Press, Cambridge.

Prince, S. D., and Goward, S. N. (1995), Global primary production: a remote sensing approach. *J. Biogeog.* 22:316–336.

Roos, B. (1969), *Analytic Functions and Distributions in Physics and Engineering*, Wiley, New York.

Ruimy, A., Saugier, B., and Dedieu, G. (1994), Methodology for the estimation of terrestrial net primary production from remotely sensed data. *J. Geophys. Res.* 99:5263–5283.

Running, S. W., and Hunt, E. R. (1993), Generalization of a forest ecosystem process model for other biomes, BIOME-BGC, and an application for global scale models. In *Scaling Ecological Process Leaf to Globe* (J. R. Ehleringer and C. B. Field, Eds.), Academic, San Diego, pp. 141–158.

Sellers, P. J. (1985), Canopy reflectance, photosynthesis and transpiration. *Int. J. Remote Sens.* 6:1335–1372.

Siewert, C., Hedstrom, G., and Chin, R. (1986), FN method for transport in a slab, UCRL Report No. 94464.

Sinclair, T. R., Schreiber, M. M., and Hoffer, R. M. (1973), Diffuse reflectance hypothesis for the pathway of solar radiation through leaves. *Agron. J.* 65:276–283.

Stokes, G. (1862), On the intensity of the light reflected from or transmitted through a pile of plates. *Proc. Roy. Soc. London* 11:5445–5556.

Vogelmann, T. C. (1989), Penetration of light into plants. *Photochem. Photobiol.* 50:895–902.

Wessman, C. A., Aber, J. D., Peterson, D. L., and Melillo, J. M. (1988), Remote sensing of canopy chemistry and nitrogen cycling in temperate forest ecosystems. *Nature* 335: 154–156.

Williams, P. C., and Norris, K. H. (1987), Qualitative applications of near-infrared spectroscopy. In *Near-Infrared Technology in the Agricultural and Food Industries* (P. Williams and K. Norris, Eds.), American Association of Cereal Chemists, St. Paul, MN, Chap. 15.